

X-ray absorption via $K\alpha$ resonance complexes in oxygen ions

Anil K. Pradhan,^{1*} Guo Xin Chen,¹ Franck Delahaye,¹ Sultana N. Nahar¹
and Justin Oelgoetz²

¹*Department of Astronomy, The Ohio State University, Columbus, OH 43210, USA*

²*Department of Chemistry, The Ohio State University, Columbus, OH 43210, USA*

Accepted 2003 February 5. Received 2003 February 5; in original form 2002 October 7

ABSTRACT

The $K\alpha$ resonance complexes in oxygen ions O I–O VI are theoretically computed, and resonance oscillator strengths and wavelengths are presented. The highly resolved photoionization cross-sections, with relativistic fine structure, are computed in the coupled channel approximation using the Breit–Pauli **R**-matrix method. A number of strong $K\alpha$ resonances are found to be appreciable, with resonance oscillator strengths $f_r > 0.1$. The $K\alpha$ resonance wavelengths of O I–O VI lie in the relatively narrow wavelength range 22–23.5 Å, and the X-ray opacity in this region should therefore be significantly affected by $K \rightarrow L$ transitions in oxygen. The results should be useful in the interpretation of soft X-ray spectra observed from *Chandra* and *XMM–Newton*.

Key words: atomic data – atomic processes – line: profiles – galaxies: Seyfert – X-rays: galaxies.

1 INTRODUCTION

K-shell excitation leads to the formation of resonance complexes in all atomic systems, with the exception of H- and He-like ions. The $K\alpha$ complex in particular, associated with the $1s \rightarrow 2p$ transition, is expected to be generally strong. The same transitions in H- and He-like ions are well known and have been observed in many *Chandra* and *XMM–Newton* sources (e.g. Branduardi-Raymont et al. 2001; Lee et al. 2001; Ness et al. 2001; Sako et al. 2002); they are bound-bound transitions and their wavelengths and oscillator strengths have been determined to very high accuracy for most elements (e.g. Drake 1979; Johnson et al. 2002). However, there are very few reliable data in the literature for resonances since they involve autoionizing states, not readily computed theoretically or observed experimentally.

We refer to lines as due to transitions between initial and final bound levels, and to resonances as due to transitions between a bound level and an interacting bound and continuum state (quasi-bound). The resonance may decay into the continuum with a finite lifetime, leading to a resonance or autoionization width in energy; it may also decay radiatively to a bound level as in the dielectronic recombination process. In astrophysical observations, with resolution usually lower than typical autoionization widths of the order of meV, line and resonance features look similar. In X-ray work, resonances are often referred to as ‘inner-shell lines’, although resonances need not be associated with inner-shell excitations alone. While the relevant transition matrix elements may be computed by

atomic structure codes by explicitly coupling the bound and continuum wavefunctions in an isolated resonance approximation, the well-established close-coupling approximation from atomic collision theory offers a complete description of the coupled wavefunctions and interference effects in resonances. Following traditional atomic physics usage, we refer to a complex as a set of lines or resonances belonging to the same principal quantum number (Eissner & Nussbaumer 1969, and references therein).

Recently, theoretical calculations of wavelengths and resonance oscillator strengths for the O VI KLL resonances (Pradhan 2000) predicted a feature at 22.05 Å that was later detected for the first time in the *Chandra* spectra of the type 1 Seyfert galaxy MCG–6-30-15 by Lee et al. (2001). Similar calculations have now been carried out for the Li-like ions, C IV, O VI and Fe XXIV (Nahar, Pradhan & Zhang 2001). These resonance oscillator strengths are needed in order to interpret the X-ray spectra of many sources. Of prime interest is the plasma in active galactic nuclei, photoionized by and surrounding the central source. We may expect that *all* ionization states of oxygen might be present in such sources, and should be identifiable through their $K\alpha$ resonance complexes, potentially leading to the determination of column densities and ionization fractions. Identifications of K- and L-shell transitions in oxygen and several other elements have also been made in the *XMM–Newton* spectra of Mrk 766 (Mason et al. 2002; Ogle et al. 2002), MCG–6-30-15 (Branduardi-Raymont et al. 2001; Lee et al. 2001), and other sources (Blustin et al. 2002; Kaastra et al. 2002). To enable the identification and analysis of such features, in this paper we present the $K\alpha$ resonance strengths derived from large-scale relativistic close-coupling calculations for the photoionization cross-sections of all ions from O I to O VI.

*E-mail: pradhan@astronomy.ohio-state.edu

2 THEORY AND COMPUTATIONS

A procedure for computing resonance oscillator strengths has been described recently by Pradhan (2000). It is well known that we may relate the line oscillator strength and the bound–free photoionization cross-section σ_{PI} to the differential oscillator strength

$$\frac{df}{d\epsilon} = \begin{cases} \frac{\nu^3}{2z^2} f_{\text{line}}, & \epsilon < I \\ \frac{1}{4\pi^2\alpha a_0^2} \sigma_{\text{PI}}, & \epsilon > I \end{cases} \quad (1)$$

where I is the ionization potential, z the ion charge, ν the effective quantum number at $\epsilon = -z^2/\nu^2$ in rydbergs (1 Ryd = 13.6 eV), and α and a_0 are the fine-structure constant and the Bohr radius, respectively. The quantity $df/d\epsilon$ describes the strength of photoabsorption per unit energy, in the discrete bound–bound region as well as the continuum bound–free region, continuously across the ionization threshold.

The quantity $df/d\epsilon$ reflects the same resonance structure as σ_{PI} in the bound–free continuum. Combining the two forms of $df/d\epsilon$ we therefore define, in the vicinity of a resonance, the integrated ‘resonance oscillator strength’ as

$$\begin{aligned} f_r(J_i \rightarrow J_f) &= \int_{\Delta E_r} \left[\frac{df(J_i \rightarrow J_f)}{d\epsilon} \right] d\epsilon \\ &= \left(\frac{1}{4\pi^2\alpha a_0^2} \right) \int \sigma_{\text{PI}}(\epsilon; J_i \rightarrow J_f) d\epsilon, \end{aligned} \quad (2)$$

where J_i , J_f represent the initial bound and continuum symmetries. Equation (2) may be evaluated from the detailed σ_{PI} for the symmetries concerned provided the resonance profile is sufficiently well delineated. In practice this is often difficult, and elaborate methods need to be employed to obtain accurate positions and profiles (the background and the peaks) of resonances. Furthermore, relativistic effects need to be included to differentiate the fine-structure components. Using the coupled-channel formulation based on the \mathbf{R} -matrix and the relativistic Breit–Pauli \mathbf{R} -matrix (BPRM) method (Burke, Hibbert & Robb 1971; Berrington, Eissner & Norrington 1995) a large number of photoionization cross-sections have been calculated for all astrophysically abundant elements including resonance structures, particularly in the Opacity Project and the Iron Project (Hummer et al. 1993; Seaton et al. 1994). We compute $df/d\epsilon$ for all ions under consideration from photoionization cross-sections from elaborate and extensive relativistic close-coupling calculations using the BPRM method. In equation (2) the resonance oscillator strength f_r is integrated over ΔE_r , the energy range associated with the autoionization width(s). An advantage of the present method is that f_r may be computed not only for an isolated resonance, but also for an overlapping complex of resonances that may not be observationally resolved.

In the close-coupling or the coupled-channel approximation the bound or resonant (e + ion) system is represented by a wavefunction expansion over coupled levels of the ‘core’ or ‘target’ ion described by configuration-interaction type eigenfunctions. The present calculations for oxygen ions employ expansions for initial ground states and $K\alpha$ resonances associated with all different (e + ion) continua (symmetry) using a number of configuration-interaction type target ion configurations, including those with a 1s hole in the K shell and a 2s hole in the L shell. The extensive list of such spectroscopic configurations, and other computational details such as (e + ion) short-range correlation configurations, will be reported elsewhere. We note that these close-coupling calculations are based on

the theory of atomic collisions, and are quite different from atomic structure calculations generally employed to compute line oscillator strengths.

The resonant transitions from the ground state of an oxygen ion into the $K\alpha$ autoionizing resonances are

$$\begin{aligned} \text{OI} : & 1s^2 2s^2 2p^4 \left({}^3\text{P}_2 \right) + h\nu \longrightarrow 1s 2s^2 2p^5 \left({}^3\text{P}_{0,1,2}^{\circ}, {}^1\text{P}_1^{\circ} \right), \\ \text{OII} : & 1s^2 2s^2 2p^3 \left({}^4\text{S}_{3/2} \right) + h\nu \\ & \longrightarrow 1s 2s^2 2p^4 \left({}^4\text{P}_{1/2,3/2,5/2}, {}^2\text{D}_{3/2,5/2}, {}^2\text{S}_{1/2}, {}^2\text{P}_{1/2,3/2} \right), \\ \text{OIII} : & 1s^2 2s^2 2p^2 \left({}^3\text{P}_0 \right) + h\nu \\ & \longrightarrow 1s 2s^2 2p^3 \left({}^5\text{S}_2, {}^3\text{D}_{1,2,3}^{\circ}, {}^1\text{D}_2^{\circ}, {}^3\text{S}_1, {}^3\text{P}_{0,1,2}^{\circ}, {}^1\text{P}_1^{\circ} \right), \\ \text{OIV} : & 1s^2 2s^2 2p \left({}^2\text{P}_{1/2}^{\circ} \right) + h\nu \\ & \longrightarrow 1s 2s^2 2p^2 \left({}^4\text{P}_{1/2,3/2,5/2}, {}^2\text{D}_{3/2,5/2}, {}^2\text{S}_{1/2}, {}^2\text{P}_{1/2,3/2} \right), \\ \text{OV} : & 1s^2 2s^2 \left({}^1\text{S}_0 \right) + h\nu \longrightarrow 1s 2s^2 2p \left({}^3\text{P}_{0,1,2}^{\circ}, {}^1\text{P}_1^{\circ} \right), \\ \text{OVI} : & 1s^2 2s \left({}^2\text{S}_{1/2} \right) + h\nu \\ & \longrightarrow 1s 2s 2p \left({}^2\text{P}_{1/2,3/2}^{\circ}, {}^4\text{P}_{1/2,3/2,5/2}^{\circ} \right). \end{aligned} \quad (3)$$

The resonances on the right-hand side of (3) autoionize into a free electron and a core ion in the ground or excited states, consistent with total fine-structure (e + ion) $J\pi$ -symmetries given as subscripts of the LS (${}^{2S+1}L^{\pi}$) terms. Whereas we locate the resonances due to all final continuum symmetries on the right-hand side, some are overlapping or are weak with little integrated resonance oscillator strength.

The monochromatic opacity arising from the $K\alpha$ resonances may be obtained from the accurate bound–free photoionization cross-sections that delineate autoionization shapes or profiles. Fine structure also needs to be included explicitly since, as shown in this work, many fine-structure components of resonances may be present. Because several coupled continuum channels contribute to each KLL resonance complex, as shown in equation (3), individual autoionization widths are not computed (and may be overlapping); instead the whole complex is delineated as a function of energy. Integration over the entire $K\alpha$ photoabsorption range therefore yields the resonance oscillator strengths reported in the next section.

Calculations for low-ionization states are more difficult than for higher states since the electron–electron correlations are stronger relative to the dominant Coulomb potential, and many more electronic configurations, both for the ion eigenfunctions and for the (e + ion) system described by continuum and bound channels, need to be considered.

Theoretical resonance spectroscopy, as formulated under the present approach, yields precise and detailed resonance positions, shapes, and oscillator strengths, complementing traditional line spectroscopy.

3 RESULTS AND DISCUSSION

Fig. 1 shows the $K\alpha$ resonant complexes of all oxygen ions, O I–O VI. The dominant components and the peak positions of resonances in each ion are shown. As mentioned above, each complex has several components; their positions may or may not overlap, depending on the exact energies of the contributing angular and spin symmetries. For example, O I and O II show one single peak because the contributing final $J\pi$ symmetries all lie at the same energy (π refers to the parity of the electronic state). On the other hand, resonances begin to spread out with ion charge in O III and O IV, which also present more complicated resonance structures. The ground level

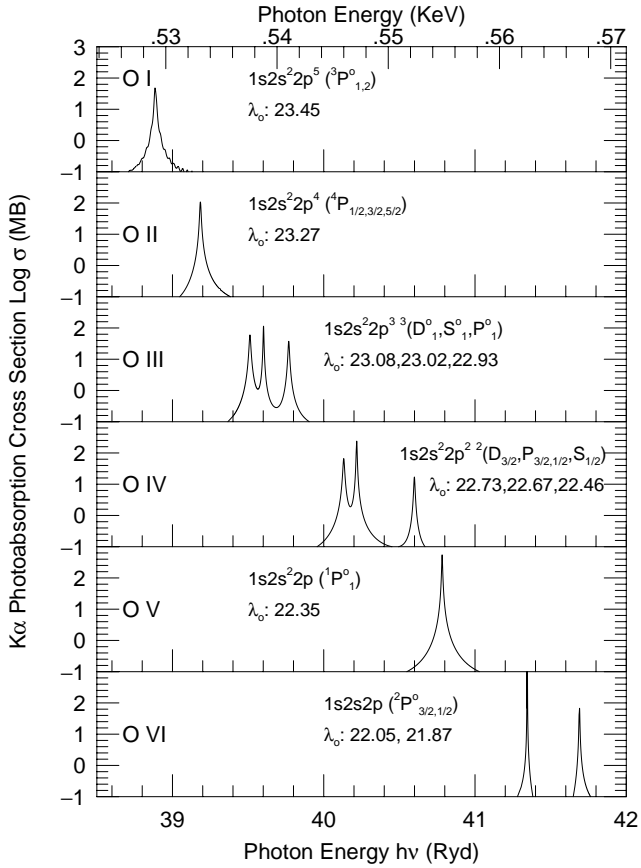


Figure 1. Photoionization cross-sections of $K\alpha$ resonance complexes in oxygen ions, O I–O VI.

of O III, $1s^2s^22p^2(^3P_0)$, photoionizes into the $J = (1)^\circ$ continuum of $1s^2s^22p^3$ with the three components shown. O V has only one final $J\pi$ ($^1P^\circ$) since the initial level is $1s^2s^2(^1S_0)$. The KLL O VI ion is a twin-component system discussed in detail in earlier work (Pradhan 2000; Nahar et al. 2001). However, the O VI resonance at 21.87 Å is about an order of magnitude weaker than the stronger one at 22.05 Å; the latter was identified in the MCG–6–30–15 spectrum by Lee et al. (2001). Most of these results for oxygen ions have been obtained for the first time (prior work is discussed below).

We note that the tentative identification by Lee et al. (2001) of the O I resonance in MCG–6–30–15 appears to be slightly higher in energy than the present value, and previous experimental and theoretical values at ~ 23.5 Å discussed by Paerels et al. (2001), who used the non-relativistic theoretical cross-sections for O I computed by McLaughlin & Kirby (1998) to analyse interstellar X-ray absorption (the theoretical model spectrum was shifted by 0.051 Å to match the measured centroid wavelength of the O I resonance). Our O II $K\alpha$ resonance is about 0.08 Å lower than that inferred from experimental data by Paerels et al. We also note that the computed wavelength for O V $K\alpha$ resonance at 22.35 Å is in good agreement with the rest wavelength of 22.334 Å recently observed with *XMM-Newton* by Blustin et al. (2002) from the type 1 Seyfert galaxy NGC 3783. The O II and O IV resonances in Fig. 1 clearly illustrate the overlapping and asymmetric nature of autoionizing resonance profiles of the respective $K\alpha$ complexes.

In Table 1 we present the $K\alpha$ resonance oscillator strengths for all oxygen ions, most with $f_r > 0.1$. It is evident from Fig. 1 that several components are nearly degenerate. The f_r given in Table 1

Table 1. $K\alpha$ resonance oscillator strengths f_r for oxygen ions.

Ion	E_r (Ryd)	E_r (keV)	λ (Å)	f_r	W_a (MeV)	σ_{\max} (MB)
O I	38.8848	0.5288	23.45	0.113	31.88	48.05
O II	39.1845	0.5329	23.27	0.184	23.21	107.7
O III	39.5000	0.5372	23.08	0.119	27.00	59.92
O III	39.6029	0.5386	23.02	0.102	12.08	114.5
O III	39.7574	0.5407	22.93	0.067	24.27	37.48
O IV	40.1324	0.5458	22.73	0.132	27.11	66.15
O IV	40.2184	0.5470	22.67	0.252	14.32	239.2
O IV	40.5991	0.5521	22.46	0.027	21.91	17.00
O V	40.7826	0.5546	22.35	0.565	14.01	549.0
O VI	41.3456	0.5623	22.05	0.576	1.090	7142.0
O VI	41.6912	0.5670	21.87	0.061	12.16	67.36

are therefore the sum over features lying approximately within 0.01 Å of each other. We also present autoionization ‘equivalent widths’ W_a (meV), together with maximum peak values σ_{\max} of the $K\alpha$ resonances (note that $f_r = W_a \times \sigma_{\max}$). It needs to be emphasized that while the values in Table 1 may be utilized to treat $K\alpha$ resonances on a par with ‘lines’, a more precise treatment is to consider the entire photoionization cross-section, up to energies encompassing the entire series of K-shell excitations, in calculating the bound–free X-ray opacity. Such calculations are more extensive and are in progress.

Another potentially important consideration is the level population in excited fine-structure levels of the ground LS term. If the source plasma is moderately dense, $N_e > 10^6 \text{ cm}^{-3}$, then the excited levels may be significantly populated. Photoabsorption therefrom would lead to additional $K\alpha$ features to augment those presented herein. These calculations are also in progress.

4 CONCLUDING REMARKS

The main conclusions of this work are as follows.

(1) The $K\alpha$ resonance strengths of oxygen ions may be used to identify and analyse soft X-ray spectral features around 0.5–0.6 keV, given the *Chandra* and *XMM-Newton* resolution of ~ 0.01 Å.

(2) Although not spatially coexistent, O VI and O VII regions may both be present and detectable via K-shell X-ray transitions from a given source. A Li-like ion, such as O VI, is easily ionized, while the ionization of a He-like ion, such as O VII, is the most energetic of all ionization states of an element and may exist in a plasma over the widest temperature range (Pradhan 1982, 1985). Thus the detection of O VI may be indicative of possibly a larger fraction of oxygen in O VII driven by recombination: $(e + \text{O VII}) \rightarrow \text{O VI}$. The O VI KLL doublet *absorption* resonances at $\lambda\lambda 22.05$ and 21.87 (Pradhan 2000) lie between the well-known forbidden (‘f’ or ‘z’), intercombination (‘i’ or ‘x, y’), and allowed (‘r’ or ‘w’) $K\alpha$ emission lines of O VII due to transitions $2(^3S_1, ^3P^\circ_{2,1}, ^1P^\circ_0) \rightarrow 1(^1S_0)$ at $\lambda\lambda 22.101, 21.804$ and 21.602 respectively (e.g. Ness et al. 2001). To augment theoretical studies, new collisional calculations for electron impact excitation of O VII have been carried out (Delahaye & Pradhan 2002). In addition, self-consistent cross-sections and rates for O VI/O VII/O VIII have been computed (Nahar & Pradhan 2003) with the same eigenfunction expansion for both photoionization and recombination, and a unified $(e + \text{ion})$ recombination scheme including both radiative and dielectronic recombination in an *ab initio* manner using the BPRM method (e.g. Nahar & Pradhan 1992; Zhang, Nahar & Pradhan 1999). The new O VII total and level-specific

recombination rates and A values, up to $n = 10$ fine-structure levels, should generally help the study of recombination lines, such as the O VII ‘He β , γ , δ , ϵ ’ identified by Sako et al. (2002) in the *XMM–Newton* spectrum.

(3) Analogous to the oxygen K α resonances at ~ 0.55 keV (22–23 Å), there are complexes corresponding to other elements such as carbon at ~ 0.3 keV, nitrogen at ~ 0.4 keV, and neon at ~ 0.9 keV. For example, a line from He-like Ne IX ($1s^2 - 1s2p$) has been identified at ~ 0.94 keV (Lee et al. 2001). Calculations are in progress for these elements.

ACKNOWLEDGMENTS

This work was partially supported by the US National Science Foundation and the NASA Astrophysical Theory Program. The computational work was carried out on the Cray-SV1 at the Ohio Supercomputer Center in Columbus Ohio.

NOTE ADDED IN PROOF

A recent experimental and theoretical study of K α photoionization of O II (Kawatsura et al. 2002) reports the resonance oscillator strengths obtained from multi-configuration Dirac–Fock (MCDF) calculations. Their combined value for the transitions $^4S_{3/2} - ^4P_{5/2}$, $^4P_{3/2}$, $^2P_{1/2}$ is 0.765, compared with the present *gf*-value of 0.736 for the total K α oscillator strength. It is expected that the other transitions not considered by Kawatsura et al. would be weaker, and if so then the present results should agree with theirs to about a few per cent. They also report that the measured position is 1.5 eV lower than the MCDF value; it appears that the energies in Table 1 and Fig. 1 for O II may be higher by a similar amount, thus providing an estimate of the uncertainties in the resonance positions in the present work.

REFERENCES

Berrington K., Eissner W., Norrington P. H., 1995, *Comput. Phys. Commun.*, 92, 290

- Blustin A. J., Branduardi-Raymont G., Behar E., Kaastra J. S., Kahn S. M., Page M. J., Sako M., Steebrugge K. C., 2002, *A&A*, 392, 453
- Branduardi-Raymont G., Sako M., Kahn S. M., Brinkman A. C., Kaastra J. S., Page M. J., 2001, *A&A*, 365, L140
- Burke P. G., Hibbert A., Robb D., 1971, *J. Phys. B*, 4, 153
- Delahaye F., Pradhan A. K., 2002, *J. Phys. B*, 35, 3377
- Drake G. W. F., 1979, *Phys. Rev. A*, 19, 1387
- Eissner W., Nussbaumer H., 1969, *J. Phys. B*, 2, 1028
- Hummer D. G., Berrington K. A., Eissner W., Pradhan A. K., Saraph H. E., Tully J. A., 1993, *A&A*, 279, 298
- Johnson W. R., Savukov I. M., Safronova U. I., Dalgarno A., 2002, *ApJS*, 141, 543
- Kaastra J. S., Steenbrugge K. C., Raassen A. J. J., van der Meer R. L. J., Brinkman A. C., Liedahl D. A., Behar E., de Rosa A., 2002, *A&A*, 386, 427
- Kawatsura K. et al., 2002, *J. Phys. B*, 35, 4147
- Lee J. C., Ogle P. M., Canizares C. R., Marshall H. L., Schulz N. S., Morales R., Fabian A. C., Iwasawa K., 2001, *ApJ*, 554, L13
- McLaughlin B. M., Kirby K., 1998, *J. Phys. B*, 31, 4991
- Mason K. O. et al., 2002, *ApJ*, 582, 95
- Nahar S. N., Pradhan A. K., 1992, *Phys. Rev. Lett.*, 68, 1488
- Nahar S. N., Pradhan A. K., 2003, *ApJS*, submitted
- Nahar S. N., Pradhan A. K., Zhang H. L., 2001, *Phys. Rev. A*, 63, 060701
- Ness J.-U., Mewe R., Schmitt J. H. M. M. et al., 2001, *A&A*, 367, 282
- Oelgoetz J., Pradhan A. K., 2001, *MNRAS*, 327, L42
- Ogle P. et al., 2002, in Jansen F. et al., eds, *ESA SP-488, New Visions of the X-ray Universe in the XMM–Newton and Chandra Era*. ESA, Noordwijk
- Paerels F. et al., 2001, *ApJ*, 546, 338
- Pradhan A. K., 1982, *ApJ*, 263, 477
- Pradhan A. K., 1985, *ApJ*, 288, 824
- Pradhan A. K., 2000, *ApJ*, 545, L165
- Sako M. et al., 2002, *ApJ*, submitted (astro-ph/0112436)
- Scott N. S., Taylor K. T., 1982, *Comput. Phys. Commun.*, 25, 347
- Seaton M. J., Yu Y., Mihalas D., Pradhan A. K., 1994, *MNRAS*, 266, 805
- Zhang H. L., Nahar S. N., Pradhan A. K., 1999, *J. Phys. B*, 32, 1459

This paper has been typeset from a $\text{\TeX}/\text{\LaTeX}$ file prepared by the author.